J|A|C|S
ARTICLES
Published on Web 05/01/2002

Synthesis and Characterization of Carbohydrate-Based Phospholipids

Geoffrey S. Hird, Thomas J. McIntosh,† Anthony A. Ribeiro,‡ and Mark W. Grinstaff*

Contribution from the Departments of Chemistry, Ophthalmology, and Biomedical Engineering, Paul M. Gross Chemical Laboratory, Duke University, and Department of Cell Biology, Duke NMR Spectroscopy Center, and Department of Radiology, Duke University Medical Center, Durham, North Carolina 27708

Received January 8, 2002

Abstract: Novel carbohydrate-based phospholipids containing two saturated C_{12} (dilauroyl ribo-phosphocholine) (DLRPC), C_{14} (dimyristoyl ribo-phosphocholine) (DMRPC), and C_{20} (diarachadonyl ribo-phosphocholine) (DARPC) carboxylic acid chains were synthesized. The physical properties of the supramolecular structures formed by these compounds were compared to those formed by their direct glycerol analogues dilauroyl phosphocholine (DLPC), dimyristoyl phosphocholine (DMPC), and diarachadonyl phosphocholine (DAPC). Modulated differential scanning calorimetry (MDSC) and X-ray diffraction data indicated that with chain lengths $\leq$14 carbons, the carbohydrate backbone increased the thermal stability of the bilayer below the phase-transition temperature (T_m) as compared to the glycerol-based lipids. With longer chains (C_{20}), the bilayer structure was destabilized as compared to glycerol-based lipids. NMR studies of a DMRPC vesicle dispersion reveal split choline headgroup signals and distinct magnetization transfer effects arising from the "inner" and "outer" surfaces of the bilayer vesicle. Modulated differential scanning calorimetry also demonstrated that glycerol- and carbohydrate-based lipids mix, as evidenced by a single intermediate T_m. In addition, carbohydrate-based lipid/cholesterol mixtures exhibited a decrease in enthalpy with an increase in cholesterol concentration. Unlike glycerol phospholipids, carbohydrate lipids were resistant to enzymatic degradation by phospholipase A_2 (PLA_2).

Introduction

Phospholipids are a major component of all prokaryotic and eukaryotic membranes.[1−3] The chemical structure of the phospholipid dictates the self-assembled bilayer structure formed, as well as the membrane physical and mechanical properties.[4−8] For example, phospholipids possessing a conical shape such as a lysolipid, with a relatively large headgroup and small monochained tail, tend to pack in spherical micelles containing hydrophobic tails on the inside and hydrophilic headgroups on the outside. Alternatively, if the phospholipid possesses a cylindrical geometry, as in the case of a diacyl phosphocholine, then bilayer structures spontaneously rearrange to form spherically self-closed liposomes in solution. Liposomes are of interest as gene transfection agents, drug delivery vehicles, ultrasound phase contrast agents, dye/fragrance carriers, and as models for biological membranes.[9−19] To optimize for a specific structural or mechanical property of the bilayer, a number of research groups are altering the structure of the phospholipid.[20−27] Current modifications of phospholipid structure are primarily limited

* To whom correspondence should be addressed. E-mail: mwg@chem.duke.edu; http://www.chem.duke.edu/~mwg/.
† Department of Cell Biology.
‡ Duke NMR Spectroscopy Center.

(1) Rosoff, M. *Vesicles*; Marcel Dekker Inc.: New York, 1996.
(2) Hanahan, D. J. *A Guide to Phospholipid Chemistry*; Oxford University Press: New York, 1997.
(3) Cevc, G., Ed. *Phospholipids Handbook*; Marcel Dekker: New York, 1993.
(4) Israelachvili, J. N. *Intermolecular and Surface Forces*; Academic Press Inc.: San Diego, 1992.
(5) Fuhrhop, J.; Koning, J. *Membranes and Molecular Assemblies: The Synkinetic Approach*; The Royal Society of Chemistry: Cambridge, 1994.
(6) Evans, E.; Skalak, R. *CRC Crit. Rev. Bioeng.* **1980**, *3*, 181−418.
(7) Tanford, C. *The Hydrophobic Effect*, 2nd ed.; John Wiley and Sons: New York, 1980.
(8) Seddon, J. M. *Biochim. Biophys. Acta* **1990**, *1031*, 1−69.
(9) Harvie, P.; Wong, F. M.; Bally, M. B. *J. Pharm. Sci.* **2000**, *89*, 652−663.
(10) Lasic, D. D.; Barenholz, Y., Eds. *Handbook of Nonmedical Applications of Liposomes*; CRC Press: New York, 1996; Vol. 4.
(11) Goldberg, B. B.; Liu, J.; Forsberg, F. *Ultrasound: Its Appl. Med. Biol.* **1994**, *20*, 319−333.
(12) Lasic, D. D. In *Vesicles*; Rosoff, M., Ed.; Marcel Dekker: New York, 1996; Vol. 62, pp 447−476.
(13) Lasic, D. D. *Liposomes in Gene Delivery*; CRC Press: New York, 1997.
(14) Felgner, J. H.; Kumar, R.; Sridhar, C. N.; Wheeler, C. J.; Tsai, Y. J.; Border, R.; Ramsey, P.; Martin, M.; Felgner, P. L. *J. Biol. Chem.* **1994**, *269*, 2550−2561.
(15) Guillaume-Gable, C.; Floch, V.; Mercier, B.; Audrezet, M.; Gobin, E.; Le Bolc'h, G.; Yaouanc, J.; Clement, J.; Abbayes, H. D.; Leroy, J.; Morin, V.; Ferec, C. *Hum. Gene Ther.* **1998**, *9*, 2309−2319.
(16) Meager, A., Ed. *Gene Therapy Technologies, Applications, and Regulations*; John Wiley & Sons: New York, 1999.
(17) Banerjee, R.; Das, P. K.; Srilakshmi, G. V.; Claudhuri, A. *J. Med. Chem.* **1999**, *42*, 4292−4299.
(18) Litzenger, D.; Huang, L. *Biochim. Biophys. Acta* **1992**, *1113*, 201−227.
(19) Needham, D.; Lasic, D. D. *Chem. Rev.* **1995**, *95*, 2601.
(20) Rui, Y.; Wang, S.; Low, P. S.; Thompson, D. H. *J. Am. Chem. Soc.* **1998**, *120*, 11213−11218.
(21) Anderson, V. C.; Thompson, D. H. *Biochim. Biophys. Acta* **1992**, *1109*, 33−42.
(22) Svenson, S.; Thompson, D. H. *J. Org. Chem.* **1998**, *63*, 7180−7182.
(23) Zalipsky, S.; Mullah, N.; Hading, J. A.; Gittelman, J.; Guo, L.; Defrees, S. A. *Bioconjugate Chem.* **1997**, *8*, 111−118.
(24) Needham, D.; Anyarambhatla, G.; Kong, G.; Dewherst, M. *Cancer Res.* **2000**, *60*, 1197−1201.
(25) Menger, F. M.; Wong, Y. *J. Org. Chem.* **1996**, *61*, 7382−7390.
(26) Geiger, H. C.; Perlstein, J.; Lachicotte, R. J.; Wyrozebski, K.; Whitten, D. G. *Langmuir* **1999**, *15*, 5606−5616.

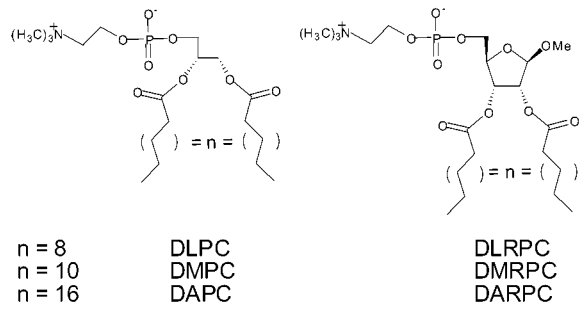

Figure 1. Chemical structures of dilauroyl phosphocholine (DLPC), dimyristoyl phosphocholine (DMPC), diarachadonyl phosphocholine (DAPC), dilauroyl ribo-phosphocholine (DLRPC), dimyristoyl ribo-phosphocholine (DMRPC), and diarachadonyl ribo-phosphocholine (DARPC).

to the hydrophilic head and hydrophobic tail groups.[25,28−30] While nonglycerol-based phospholipids such as sphingolipids[2] occur in nature, synthetic structural variations or complete substitutions of the backbone are less common with many of the chemical modifications retaining the basic glycerol three-carbon unit (e.g., cyclopentane-based phospholipids)[31] and the phosphonolipids.[32,33] These modified phospholipids exhibit different physical properties from their glycerol-based analogues, indicating the importance of backbone on bilayer structure. We are interested in the effect on vesicle structure and mechanical property when ribose is substituted for the conventional glycerol backbone.

We previously showed that the carbohydrate-based phospholipid, dilauroyl ribo-phosphocholine (DLRPC), possesses a greater phase-transition temperature and enthalpy, as compared to dilauroyl phosphocholine (DLPC).[34] In this study, we selected three chain lengths spanning from C_{12} to C_{20} to characterize and develop the structure−property relationships for this class of phospholipids. Herein we report the synthesis and physical properties of dimyristoyl ribo-phosphocholine (DMRPC) and diarachadonyl ribo-phosphocholine (DARPC), and discuss the physical property relationships between these new carbohydrate-based C_{12}, C_{14}, and C_{20} phospholipids and the corresponding glycerol analogues (Figure 1).

Results and Discussion

Synthesis of Carbohydrate-Based Phospholipids (DLRPC, DMRPC, and DARPC). Methyl-2,3-di-*O*-lauroyl-β-D-ribo-5-phosphocholine, **5** (DLRPC), methyl-2,3-di-*O*-myristoyl-β-D-ribo-5-phosphocholine, **8** (DMRPC), and methyl-2,3-di-*O*-arachadonyl-β-D-ribo-5-phosphocholine, **11** (DARPC), were synthesized as shown in Scheme 1. The first step involved protecting the primary hydroxide of **1** using trityl chloride. Purification of **2** was accomplished by silica gel column chromatography in 87% yield with an eluent of 3% methanol/chloroform. Next, a DCC coupling with DMAP and lauric/myristic/arachadonic acid in DMF afforded compounds **3**, **6**, or **9**, respectively. These intermediates were purified on a silica gel column and then immediately dissolved in aqueous acetic acid to remove the trityl protecting group. Compounds **4**, **7**, and **10** were subsequently purified by silica gel column chromatography with an overall yield of 88, 49, and 36% from **2**, respectively. The synthesis of compounds **5**, **8**, and **11** was accomplished by first reacting **4**, **7**, or **10** with 2-cyanoethyl-*N*,*N*′-diisopropylchlorophosphoramidite followed by addition of choline chloride in the presence of tetrazole. The phosphorus(III) compound was subsequently oxidized to phosphorus(V) by I_2. Finally, the cyanoethyl protecting group was removed by dissolving the mixture in 0.14 M (aq) TEA and stirring for 3 h at room temperature. Compound **5** or **8** was isolated after alumina (72/28 chloroform/methanol − 69/27/4 chloroform/methanol/H_2O), Sephadex G-10 size exclusion (50/50 chloroform/methanol), and reverse-phase C-18 Sep Pak chromatography (10/90 methanol/chloroform). The overall yield for these three steps (d−f) was 33 and 22%, respectively. Because **11** possesses longer chains, its purification was slightly different; **11** was dissolved in benzene, and the impurities were removed by filtration. The benzene solution was concentrated to a minimum before layering with MeOH and refrigerating overnight. The resulting precipitate was filtered from solution and purified using a G-10 size exclusion column in 50/50 $CHCl_3$/MeOH. Finally, a neutral alumina column (72/28 $CHCl_3$/MeOH − 69/27/4 $CHCl_3$/MeOH/H_2O) was used to isolate **11** in 5% yield.

Scheme 1. Synthetic Scheme for Bis-(2,3-lauroyl)-1-methoxy-5-(phosphocholine)-ribose (DLRPC), Bis-(2,3-myristoyl)-1-methoxy-5-(phosphocholine)-ribose (DMRPC), and Bis-(2,3-arachadonyl)-1-methoxy-5-(phosphocholine)-ribose (DARPC)[a]

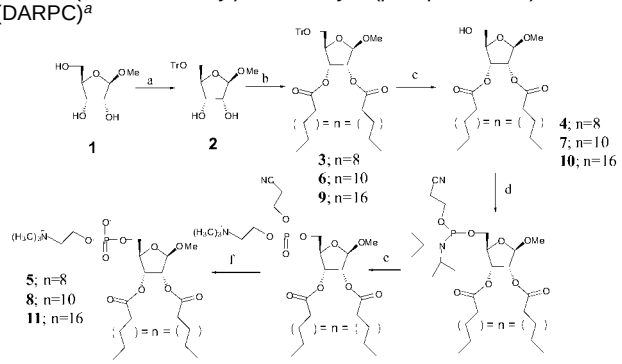

[a] Key: (a)TrCl, C_5H_5N, 3 h, 120 °C; (b) DCC, DMAP, lauric/myristic/arachadonic acid, DMF, 48 h, 60 °C; (c) acetic acid, H_2O, 12 h, 50 °C; (d) 2-cyanoethyl-*N*,*N*′-diisopropylchlorophosphoramidite, DiPEA, CH_2Cl_2, 2 h, 22 °C; (e) (i) tetrazole, choline chloride, 22 °C, 7 h, (ii) I_2, ACN, 3 h, 22 °C; (f) TEA (aq), 3 h, 22 °C.

Supramolecular Structures. DLRPC, DMRPC, and DARPC self-assemble into liposome-like structures in aqueous solution. For example, a light micrograph of DMRPC hydrating is shown in Figure 2 (bar = 50 microns). To obtain this micrograph, DMRPC is first deposited on a slide, and water is added. After incubation at 40 °C, vesicle structures bud off the solid, and these myelin figures form rapidly as the lipid rehydrates. Vesicles, most likely multilamellar, are released from the solid and are the spherical structures present in solution. Such structures are termed carbohydro-liposomes or carbohydrosomes.[34] The possible formation of micelles cannot be ruled out, since such structures are not observable at this resolution.

Alternatively, vesicles can be prepared using a high-pressure extrusion technique. This technique affords vesicle sizes from 0.05 to 15 μm. Extruding DMRPC through a 200 nm polycar-

(27) Guillod, F.; Greiner, J.; Riess, J. G. *Chem. Phys. Lipids* **1995**, *78*, 149−162.
(28) Menger, F. M.; Chen, X. Y. *Tetrahedron Lett.* **1996**, *37*, 323−326.
(29) Wang, G.; Hollingsworth, R. I. *J. Org. Chem.* **1999**, *64*, 4140−4147.
(30) Sommerdijk, N. A. J. M.; Hoeks, T. H. L.; Synak, M.; Feiters, M. C.; Nolte, R. J. M.; Zwanenburg, B. *J. Am. Chem. Soc.* **1997**, *119*, 4338−4344.
(31) Hancock, A. J. *Methods Enzymol.* **1981**, *72*, 640−672.
(32) Engel, R. *Chem. Rev.* **1977**, *77*, 349−367.
(33) Bittman, R. In *Lipid Synthesis and Manufacture*; Gunstone, F. D., Ed.; CRC Press: Boca Raton, FL, 1999; pp 185−207.
(34) Hird, G. S.; McIntosh, T. J.; Grinstaff, M. W. *J. Am. Chem. Soc.* **2000**, *122*, 8097−8098.

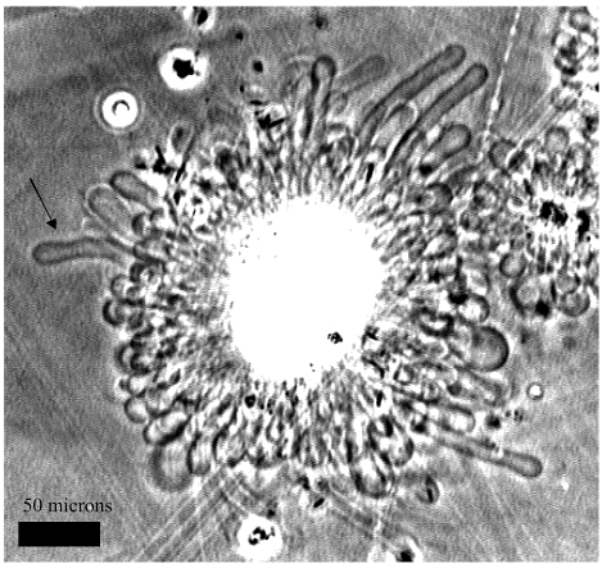

Figure 2. Light micrograph of rehydrating DMRPC at 40 °C (bar = 50 μm). The arrow points to a myelin figure.

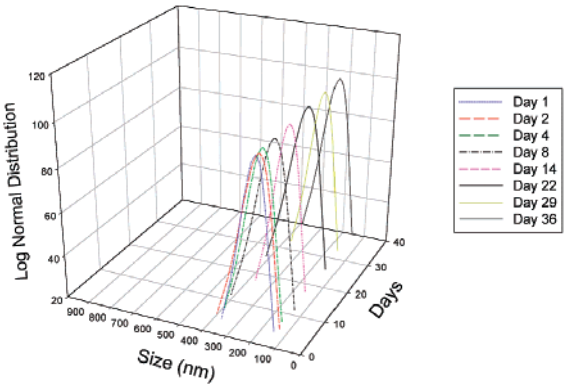

Figure 3. Stability of DMRPC carbohydro-liposomes over time at 22 °C.

bonate filter at 21 °C rendered vesicles with an average particle size of 197 nm (fwhm = 69 nm). The vesicles are stable at 22 °C with no significant change in vesicle size for more than 30 days as shown in Figure 3.

Thermal Analysis. The phase-transition temperatures (T_m) of the bilayers formed by DLRPC, DMRPC, and DARPC were determined by modulated differential scanning calorimetry (MDSC). In a typical experiment, 1 mg of lipid and 10 μL of water were hermetically sealed in an aluminum pan. Phase-transition temperatures of 15.75 ± 0.05, 29.6 ± 0.3, and 63.5 ± 0.6 °C were observed for DLRPC, DMRPC, and DARPC, respectively (Figure 4). The corresponding transition enthalpies for DLRPC, DMRPC, and DARPC are 3.3, 6.1, and 5.1 kcal/mol, respectively (Figure 5). DSC traces for DMPC and DMRPC are shown in Figure 6. The phase transitions for the carbohydrate-based lipid systems were all broader (~10 °C; fwhm = 4.1 °C) than the phase transitions observed for the corresponding glycerol-based lipids (~2 °C; fwhm = 0.4 °C). The pretransition for DMPC is observed in the heat flow trace. The broad phase transition of DMRPC collected on heating as observed in the heat flow trace has a maximum at approximately 30 °C with a shoulder at approximately 4 °C lower in temperature. These two broad peaks are slightly more separated (7 °C) on the cooling trace. Three possible explanations for the broad phase transition are the existence of extra phases, a lack

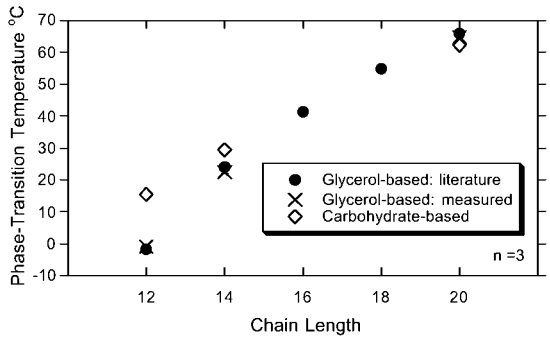

Figure 4. Phase-transition temperature (T_m, °C) vs lipid chain length.

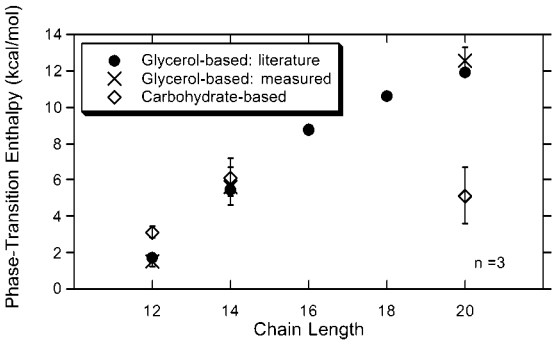

Figure 5. Phase-transition enthalpy (kcal/mol) vs lipid chain length.

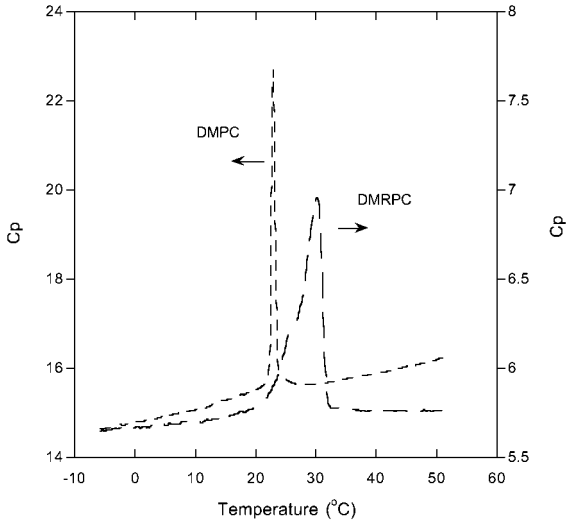

Figure 6. DSC trace of DMPC and DMRPC.

in cooperativity between the lipid molecules, or impurities. HPLC analysis showed only a single peak for the carbohydrate lipid, suggesting the first two possibilities are more likely.

DLRPC exhibits a T_m of 15.75 °C, 16 °C higher than the T_m of the glycerol analogue DLPC (−1.1 ± 0.8 °C) (see Figure 4). A melting temperature of 29.6 °C is observed for DMRPC. This T_m is approximately 6 °C higher than the phase transition of DMPC (23.5 °C).[42] The increase in T_m for both DLRPC and

(35) McIntosh, T. J.; Simon, S. A.; MacDonald, R. C. *Biochim. Biophys. Acta* **1980**, *597*, 445−463.
(36) McIntosh, T. J. *Biophys. J.* **1980**, *29*, 237−246.
(37) Weinstein, J. N.; Ralston, E.; Leserman, L. D.; Klausner, R. D.; Dragsten, P.; Henkart, P.; Blumenthal, R. In *Liposome Technology*; Gregoriadis, G., Ed.; CRC Press: Boca Raton, 1984; Vol. 3, pp 183−204.
(38) Yuan, W.; Berman, R. J.; Gelb, M. H. *J. Am. Chem. Soc.* **1987**, *109*, 8071−8081.
(39) Deems, R. A.; Dennis, E. A. *Methods Enzymol.* **1981**, *71*, 703−710.
(40) Kawana, M.; Kuzuhara, H.; Emoto, S. *Bull. Chem. Soc. Jpn.* **1981**, *54*, 1492−1504.

DMRPC indicates a more stable state below the T_m as compared to the glycerol analogues. Increased bilayer stability from replacing glycerol with ribose is a likely consequence of enhanced carbohydrate−carbohydrate and chain−chain interactions within the bilayer. The decrease in T_m difference between the carbohydrate and glycerol systems as the chain length increases from C_{12} to C_{14} is consistent with increased hydrocarbon chain packing reducing the contribution from the ribose in the bilayer. Interestingly, DARPC possesses a melting temperature of 63.5 °C which is slightly below the phase-transition temperature of DAPC (66 °C).[42] For this C_{20} analogue, DARPC, the similarity in T_m to DAPC is not entirely unexpected since tail−tail interactions are a major contributor to T_m when the tail length is long.

At the phase-transition temperature, the bilayer transforms from the gel to disordered liquid crystalline phase in glycerol-based phospholipids such as DLPC, DMPC, and DAPC. This endothermic process is observed as two discrete events. A small pretransition peak, corresponding to the conversion from a lamellar gel ($L_{\beta'}$) phase to a rippled gel ($P_{\beta'}$) phase, occurs below a larger sharp main transition peak corresponding to conversion of the $P_{\beta'}$ phase to the liquid crystalline L_α phase.[43] The temperature at which the pretransition exists as well as the enthalpy of the transition both change as a function of tail length. This presence of two well-defined phase transitions is not observed for the carbohydrate-based lipids, as discussed earlier.

The relationship between the enthalpy of phase transition and the hydrocarbon chain length for the glycerol-based phospholipids is shown in Figure 5. The literature values for the glycerol-based phospholipids (●) as well as our experimentally determined data for the glycerol-based phospholipids (×), and for the novel carbohydrate-based (◇) phospholipids, are also shown in Figure 5. The enthalpy of DLRPC is 3.3 ± 0.3 kcal/mol and is approximately double the enthalpy observed for DLPC (1.5 kcal/mol). The enthalpy of transition for DMRPC is 6.1 ± 1.0 kcal/mol and is similar to the enthalpy for DMPC (measured 5.6 ± 1.1 kcal/mol; lit. 5.9 ± 0.6 kcal/mol).[42] As the hydrocarbon chain length increases from C_{12} to C_{14}, the phase-transition temperatures and enthalpies of the carbohydrate-based lipids approach those of the glycerol-based lipids. This is consistent with chain−chain interactions becoming more important as chain length increases, reducing the influence of backbone modification on enthalpy. The T_m's of DAPC and DARPC are similar, but the enthalpy of the carbohydrate-based DARPC is lower than that of DAPC. The enthalpy of DAPC is 12.6 ± 0.7 kcal/mol (lit. = 11.9 kcal/mol),[42] while DARPC, the carbohydrate analogue, possesses an enthalpy of 5.1 ± 1.5 kcal/mol. The lower enthalpy for DARPC indicates the carbohydrate backbone is destabilizing the bilayer membrane, and this likely reflects a decrease in the collective order of the bilayer. The interaction of cholesterol with a bilayer affords a similar consequence, where the T_m remains constant but the enthalpy decreases with increased mol % cholesterol.[44]

In nature, cell membranes contain a mixture of different phospholipids. The ability of phospholipids to mix with each other can be investigated with MDSC. If two lipids mix without forming separate domains, then a single intermediate peak is observed between their respective phase-transition temperatures. If mixing is incomplete, two separate phase-transition temperatures corresponding to the two fractions are observed. Although DMPC and DMRPC as well as DLPC and DLRPC possess chemically and structurally different backbones, a single mixed bilayer is formed. For example, lipid mixtures with a single transition temperature between 29 (100% DMRPC) and 23.5 °C (100% DMPC) are formed by simply varying the DMPC/DMRPC ratios, illustrating that DMRPC mixes with DMPC to form mixed lipid bilayers (Figure 7).

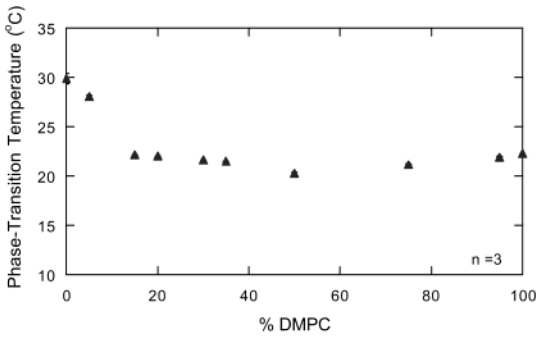

Figure 7. Phase-transition temperature (T_m, °C) vs DMPC/DMRPC mol % ratios.

X-ray Diffraction Studies. To further characterize the bilayer structures formed by DLRPC, DMRPC, and DARPC, X-ray diffraction data were collected. DLRPC and DMRPC exhibited similar phases below and above the T_m. For DLRPC at 10 °C, patterns with wide-angle reflections at 7.7, 6.1, 4.9, 4.6, and 3.9 Å were observed. For DMRPC at 22 °C, X-ray patterns consisted of several sharp wide-angle reflections at 7.74, 6.2, 4.1, and 3.9 Å.

These X-ray data are consistent with hydrocarbon chains crystallized in the plane of the bilayer;[45] this is commonly called an L_c phase. Such crystalline hydrocarbon chain packing is not typically observed with glycerol-based phospholipids below their phase-transition temperature.[42] This crystalline chain packing indicates a stable bilayer arrangement within the carbohydrate-based vesicle below the phase-transition temperature. The increase in T_m and enthalpy observed for DLRPC and DMRPC as compared to DLPC and DMPC also supports this conclusion.

X-ray diffraction patterns of DARPC at 22 °C reveal the effect of longer chains on bilayer packing. Wide angle reflections are observed at 4.1 and 3.8 Å. These data indicate a gel phase similar to that of DAPC instead of an L_c phase as seen in DLRPC and DMRPC. The bilayer formed by DARPC is similar to the bilayers formed by glycerol-based phospholipids. Because the phase transition is from a gel-liquid crystalline phase, the enthalpy is expected to be lower as compared to the change from a L_c-liquid crystalline phase.[42] The enthalpy of transition for DARPC is approximately one-half that exhibited for the glycerol-based DAPC (see Figure 8). This suggests that the carbohydrate backbone is likely destabilizing the gel state relative to the glycerol analogues by disrupting the bilayer or affording a decrease in cooperativity between the long-chain phospholipids in the bilayer.

(41) Browning, J. L. In *Liposomes: From Physical Structure to their Applications*; Knight, C. G., Ed.; Elsevier/North-Holland Biomedical Press: New York, 1981; Vol. 47, pp 189−242.
(42) Marsh, D. *CRC Handbook of Lipid Bilayers*; CRC Press: Boca Raton, FL, 1990.
(43) Silvius, J. R. *Chem. Phys. Lipids* **1991**, *57*, 241−252.
(44) McMullen, T. P. W.; Lewis, R. N. A. H.; McElhaney, R. N. *Biochemistry* **1993**, *32*, 516−522.
(45) Blaurock, A. E.; McIntosh, T. J. *Biochemistry* **1986**, *25*, 299−305.

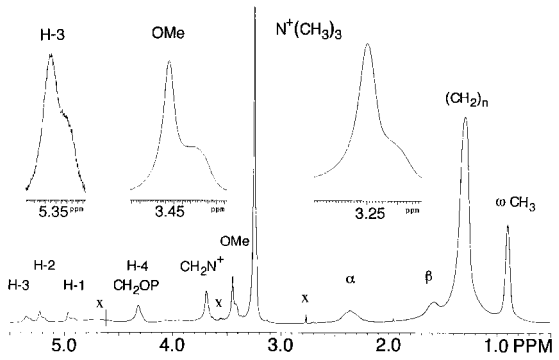

Figure 8. 600 MHz proton NMR spectra of DMRPC vesicles in D_2O at 39 °C. The expanded spectra in the insets show the splitting for the $N^+(CH_3)_3$, OMe, and ribose H-3 resonances. X indicates residual HOD or impurity resonances.

NMR Studies of the Bilayer. Figure 8 shows the NMR resonances at 600 MHz of the choline, ribose, and acyl protons of a freshly sonicated vesicle bilayer dispersion of DMRPC in D_2O. The NMR assignments for this sugar-based phosphocholine were derived from 2-D COSY from the assignments for methyl-2,3-di-*O*-lauroyl-β-D-ribo-5-phoshocholine in CD_3CN,[34] and from the literature for glycerol-based phosphocholine lipids such as egg phospatidylcholine.[46−51] The terminal choline $N^+(CH_3)_3$ signal for the DMRPC vesicles is seen to be split into two resonances about 11 Hz apart, which is identical to the splitting observed for the terminal choline $N^+(CH_3)_3$ signal of unilamellar, sonicated egg phosphocholine vesicles at 600 MHz field.[48] This splitting of the $N^+(CH_3)_3$ headgroup signal of phosphocholine (and other glycerol-based phospholipids) arises from the headgroup signals in both the interior and the exterior monolayer of the phosphocholine liposome bilayer.[46−49]

In addition to the splitting of the terminal $N^+(CH_3)_3$ signal, the ribose OMe and three individually resolved ribose resonances of the DMRPC vesicles are also split into two signals. The line shapes of the ribose signals are very similar to that of the N-terminal headgroup. In each case, the lowfield signal attributed to the "outer" layer is more intense and narrow, while the upfield signal associated with the "inner" layer is less intense and broad. Analysis of the integrated intensities gives a ratio of 1.45:1.00 for the "outer" to "inner" DMRPC signals. The chemical shift splittings for the ribose H-1, H-2, H-3, and OMe signals are ~32, 24, 21, and 20 Hz, respectively, or approximately a factor of 2 more pronounced than that of the terminal choline $N^+(CH_3)_3$ signal. The choline CH_2OP and ribose H-4 protons resonate coincidentally as a broad, overlapped signal. The choline CH_2N^+, the α, β and main methylene moieties, and the ω methyl group of the hydrophobic myristoyl chains appear as single, broad resonances for our ribose-based vesicle dispersion. Two previous papers report split choline CH_2N^+, CH_2OP, acyl CH_2, and ω methyl groups for dipalmitoyl- and dimyristoyl-phosphatidyl choline vesicles,[52,53] but, in general, most of the glycerol-based liposomes show broad unresolved choline CH_2N^+, choline CH_2OP, and acyl chain resonances.[52,54]

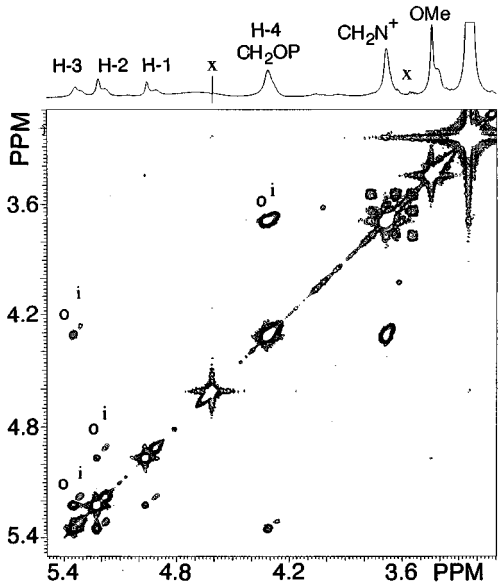

Figure 9. Expanded two-dimensional $^1H-^1H$ COSY spectra at 600 MHz of DMRPC vesicles in D_2O at 39 °C. X indicates residual HOD or impurity resonances. The cross-peaks from DMRPC molecules in the "inner" and "outer" layer are indicated with an i and *o*.

On the basis of the ^1H NMR spectrum of DLRPC in CD_3CN, the ribose H-5 protons are expected to resonate near 3.8 ppm. The NMR spectrum of the DMRPC vesicles shows no detectable resonances in the 3.8−3.9 ppm region, indicating that the H-5 signals are too broad to be observed and the backbone region near H-5 is relatively immobile.

The ribose-based liposomes were sufficiently long-lived for a 2-D NMR experiment. The expanded 2-D COSY spectrum shown in Figure 9 manifests the coherence pathways of magnetization transfer in the lipid resonances. The terminal $N^+(CH_3)_3$ and OMe signals are resonances with singlet character and show no off-diagonal COSY cross-peaks. They are split due to the contributions from DMRPC molecules in the "outer" and "inner" layers of the carbohydro-liposome. The ribose anomeric H-1 resonance is split into the tall, narrow lowfield signal at 4.97 ppm arising from DMRPC molecules in the "outer" layer of the vesicle, and the short, broad upfield signal at 4.91 ppm arising from DMRPC molecules in the "inner" layer of the vesicle. A strong and a weak off-diagonal coherence cross-peak are, respectively, observed from the 4.97 and 4.91 ppm H-1 resonances to ribose H-2 signals at 5.23 and 5.19 ppm, which correspond to the tall, narrow lowfield and short, broad upfield H-2 resonances. The 5.23 and 5.19 ppm H-2 signals, in turn, respectively show a strong and a weak coherence cross-peak to the tall and short ribose H-3 signals at 5.35 and 5.31 ppm. The two H-3 resonances then exhibit strong and weak coherence cross-peaks to the ribose H-4, which is not resolved in the one-dimensional NMR spectrum due to the coincidental overlap with the choline CH_2OP near 4.31 ppm.

The remaining 2-D coherence connectivity is from the choline CH_2OP to the choline CH_2N^+ signal near 3.69 ppm. Note that

(46) Jendrasiak, G. L. *Chem. Phys. Lipids* **1973**, *9*, 133−146.
(47) Jendrasiak, G. L.; Smith, R.; Ribeiro, A. A. *Physiol. Chem. Phys. Med. NMR* **1991**, *23*, 1−11.
(48) Jendrasiak, G. L.; Smith, R.; Ribeiro, A. A. *Biochim. Biophys. Acta* **1993**, *1145*, 25−32.
(49) Kostelnik, R. J.; Castellano, S. M. *J. Magn. Reson.* **1973**, *9*, 291−295.
(50) McLaughlin, A. C. *Magn. Reson.* **1982**, *49*, 246−256.
(51) Bystrov, V. F.; Dubrovina, N. I.; Barsukov, L. I.; Bergelson, L. D. *Chem. Phys. Lipids* **1971**, *6*, 343−347.
(52) Schuh, J. R.; Banerjee, U.; Muller, L.; Chan, S. I. *Biochim. Biophys. Acta* **1982**, *687*, 219−225.
(53) Neumann, J. M.; Zachowski, A.; Tran-Dinh, S.; Devaux, P. F. *Eur. Biophys. J.* **1985**, *11*, 219−223.
(54) Sheetz, M. P.; Chan, S. I. *Biochemistry* **1972**, *11*, 4573−4581.

this connectivity is highly skewed and asymmetric, manifesting the presence of two overlapped and unresolved "outer" and "inner" cross-peaks. The 1-D CH_2N^+ signal of egg phosphocholine vesicles has previously been resolved into "inner" and "outer" signals with the addition of anion probes.[46−48] In summary, the COSY data show that the contributions of coherence transfer are localized to DMRPC molecules within each bilayer; that is, coherence transfer effects occur in DMRPC molecules in the inner layer of the vesicle independent of effects in DMRPC molecules in the outer layer, and vice versa.

Loss of the ribose H-5 proton signal is consistent with a decrease in the backbone flexibility arising from replacement of the glycerol backbone of a phospholipid with a constrained cyclic sugar ring such as ribose. In addition, the spacing between the choline headgroup and the acyl tails is increased due to the larger ribose backbone. This, in turn, could lead to larger differences in the radii of curvature of the inner and outer monolayers for the carbohydro-liposomes as compared to liposomes. If this is indeed the case, then the packing effects that give rise to the difference in the chemical shifts of the "inner" and "outer" surfaces of the bilayer vesicle could become more pronounced at the sugar backbone in line with our current observations. All together, the NMR data suggest that the outer layer of a DMRPC vesicle is similar to the outer layer of a DMPC vesicle, while the inner layer is structurally different. One interpretation of these data is that the ribose backbone and its inherently restricted conformation have greater difficulty accommodating the imposed structure of the inner layer, which has a smaller radius of curvature, as compared to a glycerol analogue.

Cholesterol Interactions with the Bilayer. Cholesterol is present at varying concentrations in biological membranes and plays a role in modifying bilayer physical properties.[55] The consequences of adding cholesterol to a bilayer were reviewed by McMullen et al.,[44] and include a broadening and eventual elimination of the cooperative gel-liquid crystal transition of the bilayer, a decrease/increase in the orientational order of the hydrocarbon chains below/above the phase transition, the expansion/condensation of the gel/liquid-crystalline bilayer, a decreased gel phase chain tilt angle, an increase/decrease in the passive permeability of the gel/liquid-crystalline phases, and a loss of a pretransition at low cholesterol concentrations. Additional studies on lipid/cholesterol bilayer mechanical properties such as critical area strain, tensile strength, and elastic area compressibility modulus demonstrated that mechanical properties are also affected by cholesterol. For example, the area expansion modulus increases with cholesterol content until reaching a plateau at 55 mol % cholesterol.[56]

Both the pre- and the main-phase transitions decrease for glycerol-based phospholipids with the addition of cholesterol. The pretransition peak disappears when the cholesterol concentration is 5−10 mol %. Higher cholesterol concentrations are necessary to completely abolish the main transition. The enthalpy of transition for saturated diacyl glycerol-based phospholipids reaches zero regardless of chain length at about 50 mol % cholesterol.[44,56−58] A similar trend is observed with carbohydrate-based lipids. As shown in Figure 10, the enthalpy

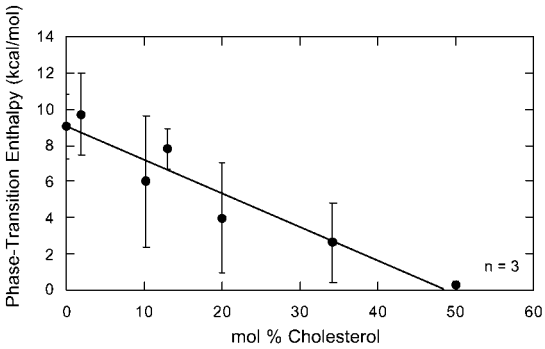

Figure 10. Phase-transition enthalpy (kcal/mol) vs mol % cholesterol in DMRPC vesicles.

is zero at 50 mol % cholesterol for DMRPC. For the glycerol-based phospholipid, cholesterol packs in the bilayer membrane with its hydroxyl group at the same level as the carbonyl groups.[59] In this structural arrangement, cholesterol primarily interacts with the tails and not the headgroup or backbone. Consequently, substitution of the glycerol by ribose is not expected to dramatically alter the location of cholesterol within the bilayer.

Phospholipids possessing tails of 17 carbons or less have a phase-transition temperature that increases as cholesterol content increases.[44] The phase-transition temperature increases as a function of cholesterol concentration and affords up to a 17 °C increase at 40 mol % cholesterol for DMPC. A different effect of cholesterol on bilayer structure is observed with long-chain glycerol derivatives. As the chain length increases to greater than 17, the phase-transition temperature decreases. A mismatch between the hydrophobic length of the cholesterol molecule and the length of the hydrophobic core of the lipid molecule determines if an increase or decrease in T_m is observed.[44] Therefore, cholesterol can either stabilize or destabilize a gel state.

For DMRPC, a slight decrease in phase-transition temperature is observed with increasing mol % cholesterol. The phase-transition temperature decreases from ∼30 °C at 0 mol % cholesterol to ∼27 °C at 35 mol % cholesterol. This result is unexpected since the tail length is less than 17 carbons. The decrease in phase-transition temperature indicates a slight destabilization of the bilayer membrane with incorporation of cholesterol. This suggests a mismatch between the hydrophobic length of DMRPC and cholesterol, disrupting the interactions between DMRPC in the bilayer. The carbohydrate backbone of our molecule may be altering the effective hydrophobic length of the bilayer area as compared to DMPC; thus DMRPC interacts with cholesterol in a manner similar to longer tail chain glycerol analogues. X-ray data on 20 mol % cholesterol/DMRPC confirm the presence of the L_c state. A repeat period of 54 Å is observed with weak reflections at crystal spacings of 3.7 and 4.8 Å.

The interaction of cholesterol with phospholipids containing modified backbones has previously been studied.[60] Bittman and Blau investigated the interaction of cholesterol with two different

(55) Yeagle, P. L., Ed. *The Biology of Cholesterol*; CRC Press Inc.: Boca Raton, FL, 1988.
(56) Needham, D.; Nunn, R. S. *Biophys. J.* **1990**, *58*, 997−1009.
(57) Ladbrooke, K. D.; Williams, R. M.; Chapman, D. *Biochim. Biophys. Acta* **1968**, *150*, 333−340.
(58) Lecuyer, H.; Bervichian, D. G. *J. Mol. Biol.* **1969**, *45*, 39−57.
(59) New, R. R. C., Ed. *Liposomes: A Practical Approach*; Oxford University Press: New York, 1990.
(60) Bittman, R.; Blau, L. *Biochemistry* **1972**, *11*, 4831−4839.

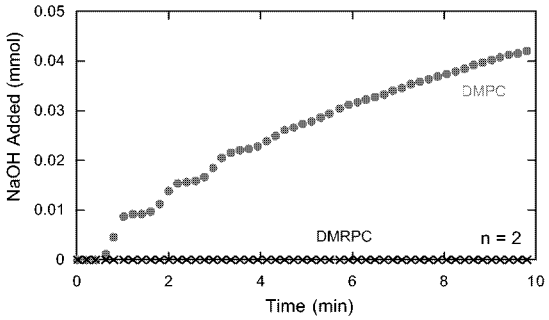

Figure 11. PLA_2 hydrolysis of DMPC and DMRPC.

types of phosphonolipids. They found that if the oxygen connecting phosphate to the glycerol backbone is replaced with a carbon, as in DL-2-hexadecoxy-3-octadecoxypropylphosphonylcholine, then the lipid is able to interact with cholesterol. If the phosphonate was attached directly to the *sn*-3 position, however, as in DL-3,4-di-octadecoxybutylphosphonylcholine, then the interaction of cholesterol within the bilayer is sterically inhibited. With the phosphonate attached directly to the *sn*-3 position, the headgroup phosphate is forced to face toward the aqueous face of the bilayer, therefore inhibiting hydrogen bonding with the terminal hydroxide of cholesterol. When the molecule is isosteric with conventional glycerol-based phospholipids as in the case of the phosphonate DL-2-hexadecoxy-3-octadecoxypropylphosphonylcholine, this hydrogen-bonding interaction remains.

Phospholipase Assays on DMRPC. Enzymes play an important role in phospholipid metabolism.[2,61] In the biological milieu, phospholipase A_2 (PLA_2) catalyzes the hydrolysis of the fatty acid from the *sn*-2 position of the glycerol backbone yielding a free fatty acid and a lyso-phospholipid. Glycerol-based phospholipids such as phosphoethanolamines and phosphocholines are known PLA_2 substrates.[2,62]

PLA_2 enzymatic activity was recorded using a pH-stat, which maintains a specific pH by adding base during the reaction which liberates fatty acid.[63] At 40 °C, DMPC was hydrolyzed with an initial average rate of 6.19×10^{-8} mol/min (std dev 6.72×10^{-10}). However, DMRPC was not hydrolyzed as shown in Figure 11.

Next, we investigated if DMRPC inhibited PLA_2 hydrolysis of DMPC. Using DMPC (5 mM) as our substrate, DMRPC was added to the reaction mixture at varying concentrations from 0.1 to 1 mM. DMRPC did not inhibit PLA_2-catalyzed hydrolysis of the *sn*-2 acyl of DMPC. Additional studies using concentrations of DMRPC up to 4 mM DMRPC did not yield a significant change in reaction rate (6.32×10^{-8} mol/min (std dev 1.36×10^{-8}) vs 6.19×10^{-8} mol/min (std dev 6.72×10^{-10})). These data indicate that DMRPC is neither a PLA_2 substrate nor a potent inhibitor.

Synthetic lipids such as the cyclopentanoid-based phospholipids have been tested as substrates for PLA_2. While a few cyclopentanoid analogues were not observed to be substrates for PLA_2, the majority of the lipids were hydrolyzed as they maintain the basic glycerol backbone.[64]

(61) Cao, Y.; Tam, S. W.; Arthur, G.; Chem, H.; Choy, P. C. *J. Biol. Chem.* **1987**, *262*, 16927−16935.
(62) Menashe, M.; Romero, G.; Bitonen, R. L.; Lichtenberg, D. *J. Biol. Chem.* **1986**, *261*, 5328−5333.
(63) Reynolds, L. J.; Washburn, W. N.; Deems, R. A.; Dennis, E. A. *Methods Enzymol.* **1991**, *197*, 3−23.

Conclusions

The carbohydrate-based analogues of DLPC, dilauroyl ribophosphocholine (DLRPC), DMPC, dimyristoyl ribo-phosphocholine (DMRPC), and DAPC, diarachadonyl ribo-phosphocholine (DARPC), possess unique chemical and physical properties. These compounds self-assemble into multibilayer structures in aqueous solution. Differential scanning calorimetry reveals larger phase-transition temperatures for DMRPC and DARPC as compared to DLRPC. This is consistent with an increase in tail chain length. The shorter tailed carbohydrate-based lipids such as DLRPC and DMRPC possess both an increased T_m and an increased enthalpy as compared to those of their glycerol-based analogue. DARPC, however, exhibits a similar T_m to DAPC but a lower enthalpy. MDSC studies indicate that the glycerol- and carbohydrate-based lipid mix as evidenced by a single intermediate phase-transition temperature. X-ray diffraction studies on DLRPC and DMRPC indicate a more ordered L_c phase below the phase-transition temperature. However, DARPC and DAPC exhibit a gel phase below the T_m. For carbohydrate-based phospholipids with C_{20} tails, the bilayer structure is less ordered as evidenced by the presence of a gel phase. A larger enthalpy per CH_2 group is observed for DLRPC and DMRPC (which have crystalline packing below T_m) as compared to DARPC (which has a gel phase below T_m). As in glycerol-based phospholipids, the length of the tail groups greatly influence bilayer physical structure and properties. NMR studies of DMRPC vesicle dispersions reveal split headgroup and backbone resonances arising from protons either in the outer or in the inner half of the bilayer, similar to vesicles from glycerol-based phopholipids. 2-D COSY data show that coherence transfer due to coupling effects occurs in DMRPC molecules in the inner layer of the vesicle independently of the coupling effects in DMRPC molecules in the outer layer. Cholesterol doping studies show that the enthalpy of transition decreases to zero at 50 mol %, comparable to the effect of cholesterol with glycerol-based phospholipids. DMRPC, unlike DMPC, is not a substrate of PLA_2. Carbohydrate-based phospholipids, such as those described here, possess several favorable attributes for evaluating lipid−lipid interactions and supramolecular structure formation. These results may also provide new insight for tailoring vesicle properties for pharmaceutical, cosmetic, and other industrial applications.

Experimental Section

(a) Materials. Instruments. One-dimensional (1-D) ^1H, ^{13}C, and ^{31}P NMR spectra characterizing synthetic intermediates and ribophospholipids were obtained on a Varian Inova 400 MHz spectrometer. Two-dimensional (2-D) COSY and HMQC spectra leading to full assignments were obtained on a Varian Unity 500 MHz spectrometer. Thin-layer chromatography (TLC) was performed on Merck KGA Silica Gel 60 (230−400 mesh; ASTM; phosphomolybdic acid). Low- and high-resolution FAB mass spectra were obtained using a JEOL JMS-SX102A mass spectrometer with 4-nitrobenzyl alcohol as the matrix and Xe as the ionizing gas. EI and CI(NH_3) mass spectra were collected on a Hewlett-Packard 5988A mass spectrometer. Modulated differential scanning calorimetry was performed on a TA Instruments 2920 modulated differential scanning calorimeter. Polycarbonate filters were purchased from Poretics Products. A Lipex extruder was used for the high-pressure extrusion experiments, and a Brookhaven Instruments

(64) Lister, M. D.; Hancock, A. J. *J. Lipid Res.* **1988**, *29*, 1297−1308

Corp. Zeta Plus Potential Analyzer was used for dynamic light scattering particle sizing. A Shimadzu RF-1501 spectrofluorimeter was used for leakage assays. Osmometry was performed on an Advanced Wide Range osmometer, Model 3W2 Advanced Instruments, Inc. (Needham Heights Mass.). C-18 Sep Pak columns were purchased from Waters Corp.

Chemicals. Chemicals were purchased from Acros, Sigma/Aldrich, Kodak, and Alfa Aesar. The oxidizing solution, 0.2 M I_2 in THF/Pyr/H_2O, was purchased from Glen Research. Sephadex G-50 was purchased from Sigma/Aldrich chemicals. All solvents indicated as dry were distilled in the laboratory over either Na/benzophenone or CaH with the exception of DMF, which was purchased from Aldrich as 99.5% pure in a Sureseal bottle.

(b) Methods. Modulated Differential Scanning Calorimetry. One to two milligrams of lipid was hermetically sealed with 9−11 μL of water in an aluminum pan. The modulation was set to ±1.00 °C every 40 s, and the pan was equilibrated at −15 °C. The temperature was increased at 0.5 °C/min to 70 °C where it was held for 2 min. The temperature was then reduced to −10 °C and held at this temperature for 2 min. This heating−cooling cycle was repeated two more times before the sample was held isothermal at −10 °C for 20 min. The data collected on the third cycle were analyzed. Integrating under the heat flow curve of the main peak afforded the enthalpy of the transition. TA Instruments Universal Analysis computer program was used to analyze the data.

X-ray Diffraction. Multilamellar suspensions of lipid were formed by hydrating 3−10 mg of compound in 1−2 mL of water at a temperature above the phase-transition temperature of the lipid. This mixture was cycled below the phase-transition temperature three times with vortexing between each cycle.[35] The mixture was centrifuged to provide a hydrated pellet of multilamellar bilayers. Pellets of DMRPC/cholesterol mixtures do not easily form usable pellets for X-ray studies. The pellet was transferred to a sealed quartz-glass X-ray capillary which was mounted in a temperature controllable chamber on a point-focus collimator. A stationary anode Jerrel-Ash generator (Jerrel-Ash Div., Fisher Scientific Co., Waltham, MA) was used to produce Cu Kα X-radiation.[36] Diffraction patterns were obtained using a flat plate film cassette loaded with Kodak DEF X-ray film. The specimen to film distance was ∼10 cm with exposure times of 2−6 h. The low angle reflections were in accordance with Bragg's law, $2d \sin\theta = h\lambda$, where λ is the wavelength (1.54 Å), d is the repeat period, h is the number of the diffraction order, and θ is the Bragg angle.

NMR Studies of Bilayer Dispersion. Biophysical NMR studies exploring the bilayer of a freshly sonicated DMRPC dispersion were performed using a Varian Inova 600 spectrometer equipped with a Sun Ultra 5 computer and 5 mm Varian probe. 1-D ^{1}H NMR spectra were recorded with a spectral window of 5.1 kHz, 8.2 s acquisition time, and digitized using 84 K points to yield a digital resolution of 0.12 Hz/pt. 2-D ^{1}H−^{1}H COSY spectra were recorded in the absolute value mode with a 5.1 kHz spectral width, 2 K points, 1 s relaxation delay, and 64 scans/increment. A total of 512 time increments was collected, and the data were processed with sine-bell weighting in the two dimensions before Fourier transformation and symmetrization to give a final 2-D matrix of 2 K by 2 K points. The Varian COSY sequence was modified to allow a long, low power transmitter pulse for solvent signal elimination at a frequency different from the nonselective high power pulses at the carrier frequency. The methyl-2,3-di-*O*-myristoyl-β-D-ribo-5-phosphocholine (DMRPC) lipid bilayers have an ordered gel to liquid crystalline phase transition near 30 °C. NMR experiments were carried out at 39 °C on a freshly sonicated vesicle bilayer dispersion of DMRPC at a concentration of 2 mg/0.6 mL D_2O.

Phospholipase A_2 Studies. The phospholipase assays were performed on a Metrohm 718 STAT Titrino pH-stat following a procedure described by Yuan et al.[38,39] Phospholipase A_2 (PLA_2) has a molecular weight of 30 000 Da and is activated by calcium. Before the assays were performed, the pH-stat was calibrated at pH 7 and pH 4. The NaOH (0.01 N) titrant was standardized by titration to pH 8.65 with a weighed amount of potassium hydrogen-phthalate in 40 mL of DI water. The lipid in methylene chloride/methanol (98/2) was transferred to a 5 mL round-bottom flask, and the solvent was removed by rotoevaporation. High vacuum then removed trace amounts of the remaining solvent. The lipid film was rehydrated with 2 mL of an aqueous solution containing Triton X-100 (40 mM) and $CaCl_2$ (10 mM) and then sonicated briefly to solubilize the lipids (DMPC; [5 mM]). Next, the solution was immersed in a temperature-controlled bath at 40 °C and stirred with a magnetic stir bar. A stream of argon was passed over the reaction mixture to prevent CO_2 absorption. A microelectrode (Metrohm 6.0224.100 pH 1−11/0−60 °C Idrolyte) was inserted through the top of the reaction vessel along with the dosing tube from the pH-stat. The reaction mixture was adjusted to a pH of 8.2 by addition of NaOH (0.1 N). Next, 0.2 units of PLA_2 (*naja naja* venom, Sigma) (0.1 units/mL) were added, and the reaction was started. The pH was allowed to drop to 8.0 and held at this value by addition of NaOH. At pH 8, the fatty acid chains hydrolyzed in the presence of PLA_2 are fully ionized, and therefore the amount of base added as a function of time provides kinetic data for the rate of the reaction. For the mixed DMRPC and DMPC experiments, the concentration of DMPC was held constant (5 mM), and the concentration of DMRPC was 0.25, 0.5, 1.0, 2.0, and 4.0 mM.

(c) Synthesis. 5-Trityl-1-β-methoxy-ribose 2. β-Methoxy ribose **1** (0.82 g, 5.01 mmol) and trityl chloride (1.63 g, 5.83 mmol) were dissolved in 100 mL of dry pyridine and heated to 120 °C for 3 h. The solvent was evaporated under high vacuum, and the resultant oil was dissolved in chloroform. The chloroform was washed with water, 0.5 N HCl, and then again with water before being dried with Na_2SO_4. Silica gel column chromatography was performed (0−3% methanol in chloroform) yielding **2** in an 87% yield (1.77 g, 4.40 mmol).[40] ^{1}H NMR ($CDCl_3$, 400 MHz, ppm): phenyl protons, 7.19−7.6 (15H, m); H(1), 4.860 (1H, s); H(3), 4.232 (1H, dd, J = 6.4 Hz, 4.8 Hz); H(4), 4.092 (1H, m); H(2), 4.0005 (1H, d, J = 4.4 Hz); OMe(1), 3.321 (3H, s); H(5), 3.246 (2H, m). ^{1}H NMR data agreed with literature values.[40]

Bis-(2,3-lauroyl)-1-methoxy-5-hydroxy-ribose, 4. 2 (1.12 g, 6.80 mmol), lauric acid (4.36 g, 21.75 mmol), and DMAP (2.66 g, 21.75 mmol) were dissolved in 175 mL of dry DMF. Next, DCC (4.49 g, 21.75 mmol) was added, and the reaction was stirred at 60 °C for 48 h to yield **3**. Acetic acid (5 mL of 5%) was added to the reaction vessel, and the white precipitate was then filtered. After removing the solvent via high vacuum, the resultant oil was dissolved in chloroform and washed with 0.5 N HCl, 5% $NaHCO_3$, and water, and then dried with Na_2SO_4 before evaporation via high vacuum. Silica gel column chromatography (10% ethyl acetate in hexane) yielded crude **3** which was dissolved in 150 mL of aqueous acetic acid and heated at 50 °C for 12 h. The solvent was removed via high vacuum, and the oil was azeotroped with toluene. Silica gel chromatography (10−30% ethyl acetate in hexane) afforded **4** in 41% yield (1.47 g, 2.78 mmol). ^{1}H NMR ($CDCl_3$, 400 MHz, ppm): H(3), 5.337 (1H, t, J = 5.6 Hz); H(2), 5.231 (1H, d, J = 4.8 Hz); H(1), 4.882 (1H, s); H(4), 4.195 (1H, m); H(5), 3.859 (2H, m); OMe, 3.410 (3H, s); H(α), 2.329 (m); H(β), 1.607 (m); $(CH_2)_m$, 1.256 (m); ω CH_3, 0.859 (t, J = 7.2 Hz). FAB mass spectrometry ($(M - H)^+$ theoretical = 528.4, observed = 527.4).

Bis-(2,3-lauroyl)-1-methoxy-5-(phosphocholine)-ribose, 5. 2-Cyanoethyl-*N*,*N*′-diisopropylchlorophosphoramidite (0.75 g, 3.35 mmol) was added dropwise to a 0 °C solution of **4** (1.47 g, 2.79 mmol) and DIPEA (0.75 mL, 3.90 mmol) in 50 mL of dry CH_2Cl_2. After stirring at 22 °C for 2 h, 1 mL of methanol was added. The solvent was removed via high vacuum after an additional hour of stirring. The resultant oil was dissolved in CH_2Cl_2 and washed with 5% $NaHCO_3$ and water before being dried with Na_2SO_4. Choline chloride (0.47 g, 3.35 mmol) was added to the flask containing the oil and dried under high vacuum overnight. Tetrazole (0.25 g, 3.62 mmol) was next added with 100 mL

of dry acetonitrile, and the reaction mixture was stirred for 7 h. Next, an oxidizing solution of 0.1 M I_2 in THF/Pyr/H_2O (approximately 20 mL) was added until I_2 remained. The solvent was removed via high vacuum yielding the intermediate (4.50 g). To remove the cyanoethyl protecting group, 0.34 g of the intermediate was dissolved in 43 mL of 0.14 M (aq) TEA and stirred for 3 h. The TEA was removed via high vacuum, and the remaining water was removed by lyophilization. Purification of **5** was achieved using alumina chromatography (72/28 chloroform/methanol − 69/27/4 chloroform/methanol/H_2O), Sephadex G-10 size exclusion chromatography (50/50 chloroform/methanol), and finally C-18 Sep Pak chromatography (10/90 methanol/chloroform). A white solid **5** was obtained in 33.5% yield for the last three steps (45.4 mg). 2-D COSY and HMQC spectrum were performed to assign the resonances observed in the ^{1}H NMR spectra. ^{1}H NMR (CD_3CN, 500 MHz, ppm): H(3), 5.205 (1H, t, J = 5.40 Hz); H(2), 5.122 (1H, dd, J = 4.80 Hz); H(1), 4.868 (1H, d, J = 1.6 Hz); H(4), 4.173 (1H, m); CH_2OP, 4.173 (1H, m); H(5), 3.848 (1H, m); H(5), 3.773 (1H, m); CH_2N^+, 3.498 (2H, m); OMe, 3.345 (3H, s); $N^+(CH_3)_3$, 3.144 (9H, s); H(α), 2.284 (4H, m); H(*β*), 1.548 (4H, m); $(CH_2)_n$, 1.266 (m); *ω* CH_3, 0.872 (t, 6.40 Hz).[41] ^{13}C NMR (CD_3CN, 125 MHz, ppm): C═O, 173.54; C═O, 173.50; C(3), 75.15; C(2), 72.53; C(1), 107.13; C(4), 81.91; CH_2OP, 59.97; C(5), 59.53; CH_2N^+, 67.48; OMe, 55.44; $N^+(CH_3)_3$, 54.80; C(α), 34.32; C(*β*), 25.401; *ω* CH_3, 12.21; $(CH_2)_n$, 30.2 (^{31}P NMR 0.067 ppm). High-resolution FAB mass spectrometry ($(MH)^+$ theoretical = 694.4659, observed = 694.4653).

Bis-(2,3-myristoyl)-1-methoxy-5-hydroxy-ribose, 7. 2 (1.22 g, 7.46 mmol), myristic acid (5.45 g, 23.86 mmol), DMAP (2.92 g, 23.86 mmol), and DCC (4.93 g, 23.86 mmol) were stirred in 150 mL of DMF for 48 h at 60 °C to afford **6**. The solution was filtered, and the resultant mixture was purified on a silica gel column with the eluent of 9/1 Hex/EtAc. Next, the solid was immediately dissolved in aqueous acetic acid and stirred at 50 °C for 12 h. The product, **7**, was subsequently purified by silica gel column chromotography (eluent 7/3 Hex /EtAc) with an overall yield of 49% for the two steps (2.12 g, 3.63 mmol). ^{1}H NMR ($CDCl_3$, 400 MHz, ppm): H(3), 5.339 (1H, t); H(2), 5.233 (1H, d); H(1), 4.888 (1H, s); H(4), 4.196 (1H, m); H(5), 3.863 (2H, m); OMe, 3.413 (3H, s); H(α), 2.331 (m); H(*β*), 1.610 (m); $(CH_2)_m$, 1.260 (m); *ω* CH_3, 0.863 (t).

Bis-(2,3-myristoyl)-1-methoxy-5-(phosphocholine)-ribose, 8. Compound **8** was prepared by first reacting **7** (0.64 g, 1.09 mmol) with 2-cyanoethyl-*N*,*N*′-diisopropylchlorophosphoramidite (0.37 mL, 1.64 mmol) and DIPEA (0.33 mL, 1.86 mmol) in 60 mL of dry CH_2Cl_2 at 0 °C. The reaction was stirred for 2 h at 22 °C under N_2. This reaction mixture was then quenched with 2 mL of MeOH, and then the solvent was removed by high vacuum. The mixture was dissolved in distilled CH_2Cl_2, and then washed with 5% $NaHCO_3$ and water before being dried with Na_2SO_4. Dried choline chloride (0.20 g, 1.42 mmol) was added to the reaction vessel. Next, the resultant mixture was dissolved in 100 mL of dry CH_3CN containing tetrazole (0.10 g, 1.42 mmol), and then stirred for 7 h. An oxidizing solution of 0.2 M I_2 in THF/Pyr/H_2O was added with stirring until the solution remained yellow indicating that the phosphorus was fully oxidized, yielding the cyanoethyl protected intermediate. This mixture was again evaporated and azeotroped with benzene. To remove the cyanoethyl protecting group, the contents of the reaction vessel were dissolved in 0.134 M (aq) TEA and stirred for 3 h at room temperature. The TEA was removed with high vacuum, and the water was removed by lyophilization. The crude product was purified by alumina column chromatography (72/28 $CHCl_3$/MeOH − 69/27/4 $CHCl_3$/MeOH/H_2O), by Sephadex G-10 size exclusion chromatography (50/50 $CHCl_3$/MeOH), followed by C-18 Sep Pak chromatography (10/90 MeOH/$CHCl_3$). Compound **8** (0.18 g, 0.25 mmol) was obtained in 22.4% yield for the last three steps d−f. 2-D COSY and HMQC spectrum were performed to assign the resonances observed in the ^{1}H NMR spectra. ^{1}H NMR (CD_3CN, 400 MHz, ppm): H(3), 5.209 (1H, t, J = 31.2 Hz); H(2), 5.120 (1H, dd, J = 2.2 Hz); H(1), 4.870 (1H, d, J = 0.8 Hz); H(4), 4.190 (1H, m); CH_2OP, 4.190 (1H, m); H(5), 3.880 (1H, m); H(5), 3.801 (1H, m); CH_2N^+, 3.513 (2H, m); OMe, 3.344 (3H, s); $N^+(CH_3)_3$, 3.141 (9H, s); H(α), 2.282 (4H, m); H(*β*), 1.542 (4H, m); $(CH_2)_n$, 1.261 (m); *ω* CH_3, 0.871 (t, 7.2 Hz). ^{13}C NMR (CD_3CN, 100 MHz, ppm): C═O, 173.62; C═O, 173.35; C(3), 75.12; C(2), 72.17; C(1), 107.15; C(4), 80.97; CH_2OP, 60.40; C(5), 59.20; CH_2N^+, 67.10; OMe, 55.75; $N^+(CH_3)_3$, 54.89; C(α), 34.52; C(*β*), 25.51; *ω* CH_3, 14.39; $(CH_2)_n$, 30.65 (^{31}P NMR 0.595 ppm). High-resolution FAB mass spectrometry ((MH^+) theoretical = 750.5285, observed = 750.5255).

Bis-(2,3-arachadonyl)-1-methoxy-5-hydroxy-ribose, 10. 2 (1.02 g, 6.20 mmol), arachadonic acid (6.19 g, 19.81 mmol), and DMAP (2.42 g, 6.20 mmol) were dissolved in 200 mL of dry DMF. DCC (4.09 g, 6.20 mmol) was added dropwise, and the reaction was stirred at 40 °C for 48 h. Next, 5 mL of 5% acetic acid was added to the reaction vessel, and the white precipitate was filtered. The resultant solution was evaporated under high vacuum before being dissolved in $CHCl_3$ and washed with 0.5 N HCl, 5% $NaHCO_3$, and water. After drying with Na_2SO_4, the solution was rotoevaporated to dryness. Silica gel column purification (9/1 Hex/EtAC) was performed. The product was dissolved in aqueous acetic acid and stirred at 50 °C for 12 h to remove the trityl protecting group. The deprotected product was purified by silica gel column chromatography (9/1 Hex/EtAC − 7/3 Hex/EtAc) to afford **10** in a 36% yield (1.60 g). ^{1}H NMR ($CDCl_3$, 400 MHz, ppm): H(3), 5.338 (1H, t); H(2), 5.235 (1H, d); H(1), 4.887 (1H, s); H(4), 4.197 (1H, m); H(5), 3.867 (2H, m); OMe, 3.415 (3H, s); H(α), 2.332 (m); H(*β*), 1.613 (m); $(CH_2)\mu$, 1.258 (m); *ω* CH_3, 0.862 (t).

Bis-(2,3-arachadonyl)-1-methoxy-5-(phosphocholine)-ribose, 11. 10 (1.18 g, 2.46 mmol) was dissolved in 45 mL of dry CH_2Cl_2, and DIPEA (0.73 mL, 4.18 mmol) was added. The reaction vessel was then chilled to 0 °C before adding 2-cyanoethyl-*N*,*N*′-diisopropylchlorophosphoramidite (0.02 mL, 3.70 mmol). The reaction was stirred for 4 h at 22 °C and subsequently evaporated under high vacuum for 1.5 h. The crude material was dissolved in dry CH_2Cl_2 and then washed with 5% $NaHCO_3$ and H_2O before being dried with Na_2SO_4. Choline chloride (0.49 g, 3.20 mmol) was azeotroped twice with toluene, dried under high vacuum overnight at 45 °C, and then added to the flask containing the intermediate. The reaction mixture was then dissolved in 94/6 CH_3CN/CH_2Cl_2, and tetrazole (0.22 g, 3.20 mmol) was added. The reaction was stirred for 12 h. Oxidation of the P(III) was accomplished using I_2 in THF/Pyr/H_2O, and the reaction was stirred for 3 h and then evaporated under high vacuum. The resultant mixture was dissolved in 113 mL of H_2O containing 2 mL of TEA and stirred for 3 h at 22 °C. The solvent was subsequently removed by lyophilization. To isolate the product, the reaction mixture was first dissolved in benzene and filtered. The benzene solution was then concentrated to a minimum before layering with MeOH and refrigerating overnight. Next, the resulting product was filtered from solution and purified using a G-10 size exclusion column in 50/50 $CHCl_3$/MeOH followed by a neutral alumina (70−230 mesh) column (72/28 $CHCl_3$/MeOH − 69/27/4 $CHCl_3$MeOH/H_2O) to afford 0.12 g (5.2% yield) of product. ^{1}H NMR (CD_3OD, 400 MHz, ppm): H(3), 5.353 (1H, t, J = 5.6 Hz); H(2), 5.214 (1H, m); H(1), 4.910 (1H, m); H(4), 4.250 (1H, m); CH_2OP, 4.280 (1H, m); H(5), 3.951 (1H, m); H(5), 3.951 (1H, m); CH_2N^+, 3.624 (2H, m); OMe, 3.390 (3H, s); $N^+(CH_3)_3$, 3.212 (9H, s); H(α), 2.341 (4H, m); H(*β*), 1.605 (4H, m); $(CH_2)_m$, 1.295 (m); *ω* CH_3, 0.860 (t, 7.2 Hz). ^{13}C NMR (CD_3OD, 100 MHz, ppm): C═O, 173.43; C═O, 173.18; C(3), 74.83; C(2), 71.81; C(1), 106.64; C(4), 80.60; CH_2OP, 62.73; C(5), 59.30; CH_2N^+, 67.11; OMe, 55.507; $N^+(CH_3)_3$, 54.72; C(α), 34.32; C(*β*), 25.12; $(CH_2)_m$, 30.41; *ω* CH_3, 14.18 (^{31}P NMR 2.22 ppm). High-resolution FAB MS (MH^+) (theoretical = 918.7099, observed = 918.7169).

Acknowledgment. This work was supported by the North Carolina Biotechnology Center (M.W.G.), the American Heart Association (M.W.G.), the Pharmaceutical Sciences NIH Training Grant (G.S.H.), NIH grant GM27278 (T.J.M.), and Duke

University. The Duke NMR Center is supported in part by NIH NCI P30-CA-14236 (A.A.R.). NMR instrumentation was funded by NSF, NIH, the North Carolina Biotechnology Center, and Duke University. The authors would like to thank Jeff Mills, Dr. David Needham, Dr. Jason Keiper, Dr. Steve Aubuchon, and Dr. Stephen Lee. M.W.G. also thanks the Pew Foundation for a Pew Scholars Award in the Biomedical Sciences, the Dreyfus Foundation for a Camille Dreyfus Teacher-Scholar, and the Alfred P. Sloan Foundation for a Research Fellowship.

Supporting Information Available: NMR spectra of DLRPC, DMRPC, and DARPC (PDF). This material is available free of charge via the Internet at http://pubs.acs.org.

JA025542Q